CRYSTAL GROWTH & DESIGN

Article

pubs.acs.org/crystal

Importance of Solvent Selection for Stoichiometrically Diverse Cocrystal Systems: Caffeine/Maleic Acid 1:1 and 2:1 Cocrystals

Tom Leyssens,*[,†] Geraldine Springuel,[†] Riccardo Montis,[†] Nadine Candoni,[‡] and Stéphane Veesler[‡]

[†]Université Catholique de Louvain, IMCN, Place Louis Pasteur 1, B-1348 Louvain-la-Neuve, Belgium

[‡]CiNaM-CNRS, Aix-Marseille Université, Campus de Luminy, F-13288 Marseille, France

Supporting Information

ABSTRACT: Phase diagrams of cocrystals often show a highly unsymmetrical nature. The solvent has an important impact on the overall aspect of these diagrams. In this paper, we show how the solvent affects the composition of the stoichiometric solid phase nucleated. Suitable conditions for nucleation and growth of a single 2:1 caffeine/maleic acid cocrystal are obtained in ethyl acetate, showing comparable solubility toward both caffeine and maleic acid. Through a full kinetic screen, we were able to identify, for the first time, reproducible conditions for the spontaneous crystallization of the 2:1 phase in solution. Furthermore, during the screening experiments, a hithertho unknown form of the 1:1 cocrystal phase was encountered. Structural X-ray diffraction analyses of both the 2:1, as well as the 1:1 polymorphic phases, show an out of plane maleic acid compound. The carboxylic acid groups are oriented in such a manner to promote intermolecular formation of hydrogen bonded synthons.

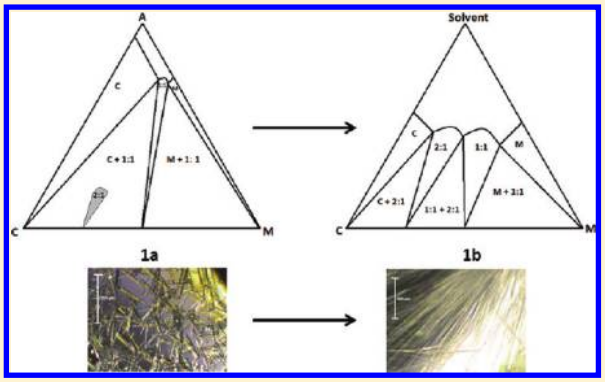

INTRODUCTION

The final solid phase of a pharmaceutical active compound (API) is essential for its physicochemical properties such as solubility, bioavailability,[1] and stability. Increasing efforts are made not only to control the solid phase but also to modify the solid phase of a given compound to yield optimal properties, so-called "crystal engineering".[2−4] Alternative polymorphs, solvates, and salts were the first to be considered as alternative phases. Moreover, over the past decade, cocrystals have received a growing interest, especially when the options of forming ionic complexes are limited[5] or ionic complexes are unstable. Generally, a cocrystal is broadly defined as "a multiple component crystal formed between compounds that are solid under ambient conditions; at least one component is molecular and forms supramolecular synthons with the remaining components."[6] Although these alternative solid phases often show interesting properties, industrial development of cocrystal applications remains limited, an observation which, in part, can be explained by the difficulty in producing these compounds on a larger scale.[2] In recent contributions, the importance of understanding the thermodynamic characteristics of a cocrystal system for the development of an upscaled crystallization process has been highlighted.[7,8] Phase diagrams are key to the development of a robust up-scaled process, but the often highly unsymmetrical nature of phase diagrams involving cocrystals explains the difficulties encountered when developing a robust process. The solvent has an important impact on the overall aspect of ternary phase diagrams involving cocrystals but also on the kinetics of phase nucleation. In this paper, the importance of the solvent for the synthesis of stoichiometrically diverse cocrystals is investigated. More specifically we show how, using basic thermodynamic considerations, the choice in solvent affects the composition of the stoichiometric solid phase nucleated.

Caffeine is a model pharmaceutical compound known to exhibit instability with respect to humidity, with the formation of a crystalline nonstoichiometric hydrate.[9,10] Because of the weakly basic imidazole nitrogen of caffeine, only one pharmaceutically acceptable salt phase has been identified so far.[11] However, given its weak basicity, and particular possibility of forming [$R^2_2(7)$] heteromeric synthons (Scheme 1), caffeine was found particularly suited for cocrystallization.[12−21]

Trask et al.[22] were the first to perform a systematic crystal engineering study of pharmaceutical cocrystals of caffeine, using dicarboxylic acids as coformers. As dicarboxylic acids can form two heterosynthons of the type shown in Scheme 1, 2:1 cocrystals (e.g., Scheme 2) were expected. However these latter were only found, when using oxalic acid or malonic acid as coformer, while other acids such as glutaric acid yielded a 1:1 cocrystal. Maleic acid showed an even more surprising result, as two stoichiometrically diverse cocrystals were identified. Formation of either the 1:1 or 2:1 caffeine/maleic acid cocrystal depended on grinding conditions used. Furthermore, no reproducible experimental conditions for the preparation of

Received: November 30, 2011
Revised: December 21, 2011

   dx.doi.org/10.1021/cg201581z | *Cryst. Growth Des.* XXXX, XXX, XXX−XXX

Scheme 1. Caffeine/Carboxylic Acid $[R^2_2(7)]$ Heterosynthon

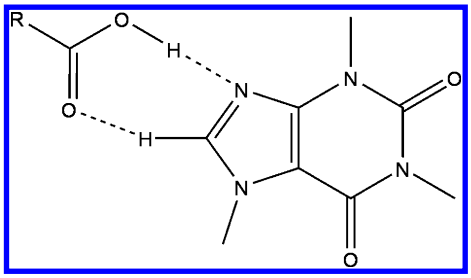

Scheme 2. Expected Caffeine/Maleic Acid 2:1 Cocrystal

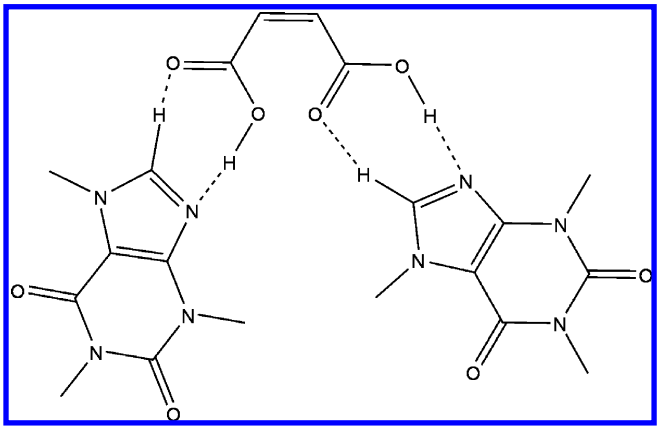

the 2:1 cocrystal in solution have been identified, and hence the structure of this latter phase remained unsolved up to now. Recently, in their attempts to grow a single 2:1 cocrystal Guo et al.[23] proclaimed the 2:1 phase to be metastable at 25 °C. In addition, they showed a ternary phase diagram involving acetone (Figure 1a), where an approximate labile zone is given for the 2:1 cocrystal (spontaneous nucleation due to high supersaturation level), within the stable zone of the 1:1 cocrystal. Although they suggest this phase could be stable at higher temperatures, no specific mention was made as to how the nature of the solvent would affect the overall ternary phase diagram.

In this paper, we used the caffeine/maleic acid system to show the importance of the solvent in the crystallization of stoichiometrically diverse cocrystals, by setting out to identify suitable conditions for nucleation and growth of a single 2:1 caffeine/maleic acid cocrystal. To achieve this goal, the solvent is chosen in such a manner to enhance the probability of nucleating the 2:1 phase on the basis of solubility considerations of the pure components of the cocrystal. We were able to grow a 2:1 crystal large enough for structural analysis in a mere two months. Moreover, during our screening experiments, we identified a new polymorph of the 1:1 cocrystal. The presence of polymorphic phases of cocrystals is important, not only for patent issues and bioavailability, but also from process and physicochemical point of views.

EXPERIMENTAL SECTION

Materials. Maleic acid (99% chemical purity) and caffeine (98.5% chemical purity) were purchased from Acros Organics and were used without further purification. Both compounds were analyzed by X-ray powder diffraction. The most stable phase of caffeine (β phase)[24,25] was used throughout this study. Ethyl acetate (HPLC grade, from VWR International) was used with no further purification.

Single Crystal X-ray Diffraction. *2:1 Cocrystal.* The intensity data were collected on a Bruker−Nonius Kappa CCD diffractometer using MoKα radiation (λ = 0.71073 Å). Data collection were performed with COLLECT,[26] cell refinement, and data reduction with DENZO/SCALEPACK.[27] The structure was solved by SHELXS-97[28] and SHELXL-97[28] was used for full matrix least-squares refinement. Non-hydrogen atoms were anisotropically refined. The hydrogen atoms were positioned geometrically and refined in the riding mode with isotropic temperature factors fixed at 1.5 times U(eq) of the parent atoms. The data have been deposited with the Cambridge Crystallographic Data Centre (No. 844797).

1:1 (FII) Cocrystal. The X-ray intensity data were collected at 120 K with a MAR345 image plate using MoKα (λ = 0.71069 Å) radiation. A crystal of approximate dimensions 0.36 × 0.33 × 0.28 mm^3 was chosen. The unit cell parameters were refined using all the collected spots after the integration process.

A total of 11 302 reflections were collected from 168 images ($\Delta\phi$ = 3°) covering four different crystal orientations. There are 2615 independent reflections (R_{int} = 6.48%). The structure was solved by direct methods SHELXS97[28] and refined by full-matrix block least-squares on F^2 using SHELXL97.[28] All non-hydrogen atoms were refined anisotropically. The hydrogen atoms were placed at calculated positions and refined isotropically with temperature factors fixed at 1.2$U_{(eq)}$ of the parent atom (1.5$U_{(eq)}$ for methyl groups). Final R-values are R_1 = 0.0591 for 2331 observed reflections (>2σ(I)); R_1 (all data) = 0.0629, wR_2 = 0.1638, S = 1.087. All data were integrated by

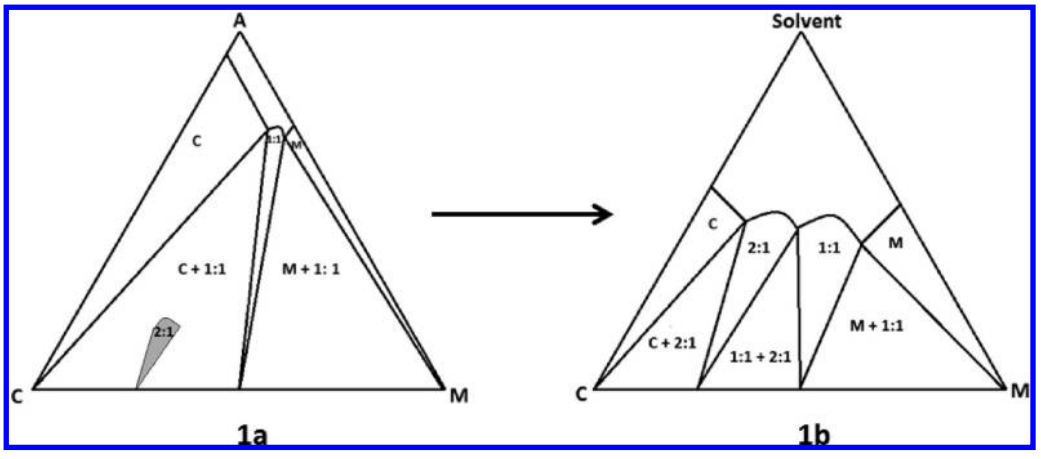

Figure 1. (a) Ternary phase diagram of caffeine and maleic acid in acetone at 25 °C in molar % (source ref 23). (b) Hypothetical phase diagram in a solvent showing comparable maleic acid and caffeine solubility. A, C, and M for acetone, caffeine, and maleic acid, respectively.

dx.doi.org/10.1021/cg201581z | Cryst. Growth Des. XXXX, XXX, XXX−XXX

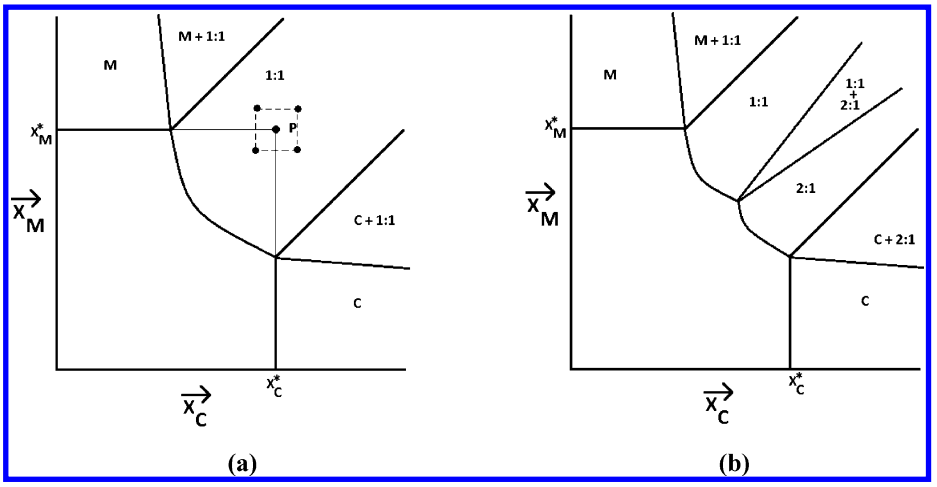

Figure 2. Phase diagram, constructed by considering concentration of caffeine on the *x*-axis and concentration of maleic acid on the *y*-axis. Zones indicate which solid phases are in equilibrium with the liquid phase. (a) Showing a 1:1 cocrystal system. (b) Showing a putative diagram of a 2:1/1:1 stoichiometrically diverse system.

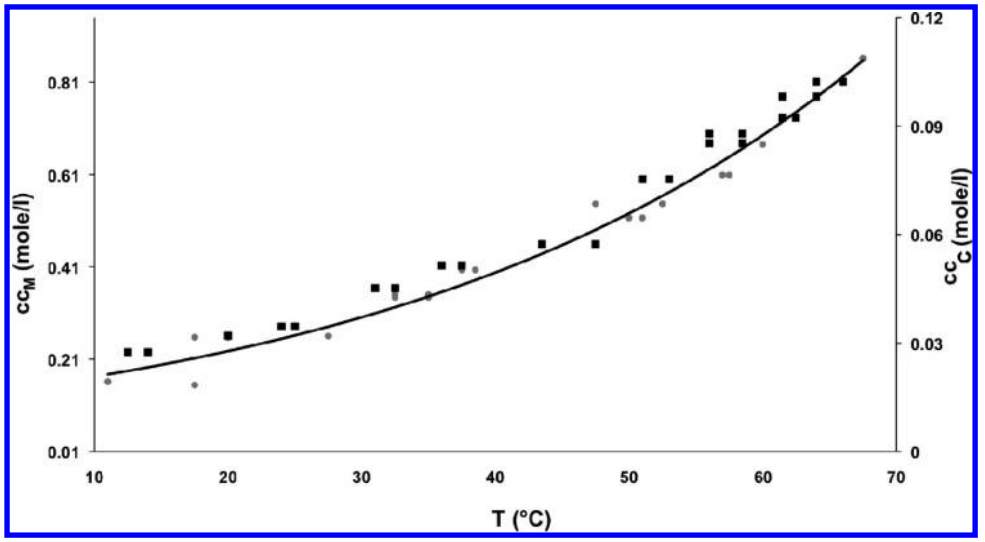

Figure 3. Solubility curve showing the concentration of maleic acid (cc_M; left axis; gray points) and caffeine (cc_C; right axis; full black squares) determined with a multiwell scanning device. Exponential fit is drawn for maleic acid.

Table 1. Initial Screen. Input Concentration in Maleic Acid (cc_M) and Caffeine (cc_C)[a]

sample	T_{ref}/T_{cryst} (°C)	cc_C (mol/L)	cc_M (mol/L)	phase
1	35/10	0.047	0.350	1:1
2	35/10	0.055	0.383	2:1
3	35/10	0.043	0.315	1:1
4	35/10	0.042	0.418	M
5	35/10	0.055	0.313	2:1
6	55/20	0.080	0.579	1:1
7	55/20	0.088	0.657	M
8	55/20	0.073	0.525	1:1 (FII)
9	55/20	0.073	0.653	M
10	55/20	0.089	0.543	2:1

[a]Samples were prepared along an experimental plan as shown in Figure 2a. Central points (1 and 6) contain caffeine and maleic acid at their respective solubility at 35 and 55°C.

chrysalis and scaled, merged, and corrected for absorption by SADABS.

The data have been deposited with the Cambridge Crystallographic Data Centre (No. 844798).

X-ray Powder Diffraction (XRPD). Transmission mode X-ray diffraction (XRD) measurements were performed with an INEL CPS 120 diffractometer equipped with a linear curved detector covering an angular domain of 120°. A Si monochromator assures focalization of the beam on the detector. Kα radiation of Cu (λ = 1.5418 Å) is used. Samples were placed in vertically positioned glass capillaries.

Differential Scanning Calorimetry (DSC). DSC measurements were performed on a DSC 821 METTLER TOLEDO. Prior to measurements, the DSC was calibrated using indium. Perforated aluminum crucibles were used for analysis. The heating rate was set at 10 °C min^{-1} over a range from 30 to 180 °C. Samples were obtained after crystallization from solution. After light grinding, a white fine powder was obtained in all cases.

Solubility Determination/Screening/Optical Microscopy. A homemade inverted microscope Multiwell screening device (available commercially – ANACRISMAT) was used for determination of the solubility curves, screening of crystallization conditions, and for optical imaging.[29] Vials are inserted into two blocks (for 1 mL vials, each block containing 12 vials) thermostatted independently by Peltier elements, and observed by an inverted microscope (Nikon Eclipse TE2000-U). The whole assembly is mounted on an X-Y translation table. Screening experiments are also performed offline, storing the vials for longer periods at given temperatures.

dx.doi.org/10.1021/cg201581z | *Cryst. Growth Des.* XXXX, XXX, XXX–XXX

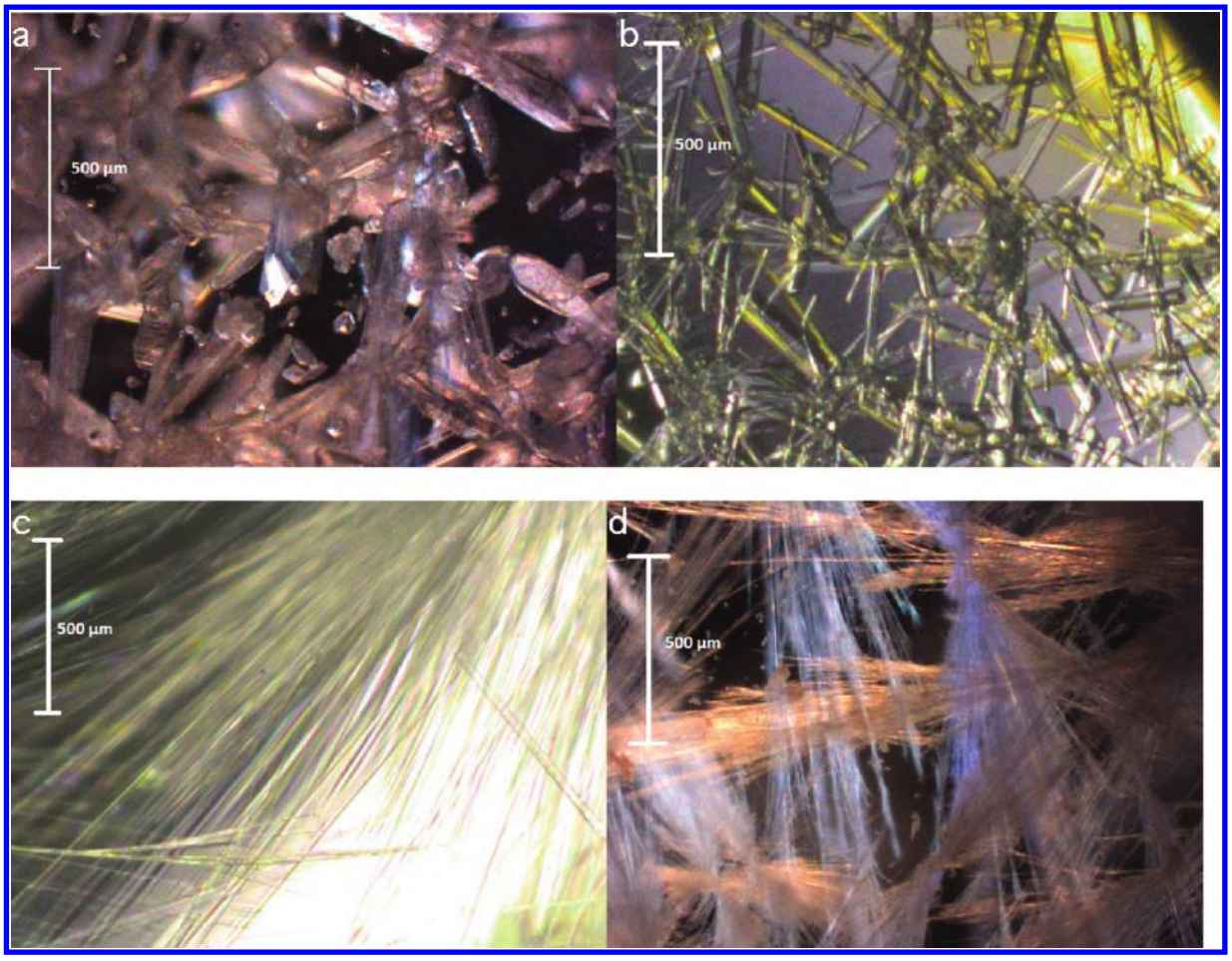

Figure 4. OM images of (a) sample 4, (b) sample 1, (c) sample 2, (d) recrystallized caffeine. Images are taken in ethyl acetate. Samples are defined in Table 1.

Solubility measurements were carried out, preparing vials at different concentrations and holding them at a given temperature. If no dissolution occurred, the temperature was increased by 1 °C, and vials were left for over 30 min, during which time they were shaken vigorously. Repeated temperature increases were applied until total dissolution occurred, at which point the temperature was noted as the dissolution temperature (T_d) for a given concentration; the equilibrium temperature (T_{eq}) is bracketed according to the following formula:

$$T_d - 1 < T_{eq} < T_d \quad (1)$$

RESULTS AND DISCUSSION

Solvent Selection. The respective interaction of each solute component of the cocrystal with the solvent often leads to asymmetric phase diagrams, as illustrated by the ternary phase diagram of the 1:1 caffeine/maleic acid cocrystal in acetone obtained by Guo et al.[23] (Figure 1a). The asymmetry is due to the strong difference in solubility between maleic acid and caffeine in acetone. Indeed, at 25 °C maleic acid is about 40 times more soluble in acetone compared to caffeine. The phase diagram presents a relatively narrow zone, in which the 1:1 cocrystal is the only stable phase in suspension. Figure 1a shows how these authors describe the 2:1 cocrystal zone as a kinetically accessible metastable zone embedded in the thermodynamic zone containing mixtures of caffeine and the 1:1 cocrystal. To achieve spontaneous crystallization of 2:1 cocrystal phase in acetone, very large supersaturation is required such as that observed during ultrasound crystallization experiments.[30]

To explain the stability of a given cocrystal composition in suspension, one needs to consider the solubility product (K_{sp}) of the cocrystal, the solubility of each component, and the solution pair wise complexation constants (K_{11}, and K_{12}).[31−33]

For 1:1 cocrystal systems, Ainouz et al. showed the size of the ternary phase diagram zone in which a pure 1:1 cocrystal solid phase is in equilibrium with a liquid phase, to depend on the relative solubility of both components. When the solubility of either one of the components strongly differs from the other, this zone can completely disapear.[34] However, this does not imply that the 1:1 cocrystal solid phase cannot be observed in solution, as nucleation of this phase could still be kinetically favored.

Extending their findings to a 1:1/2:1 cocrystal system, and using a graphic approach, the zone where the 2:1 cocrystal is in equilibrium with a liquid phase could become more easily accessible when a more symmetric aspect is given to the phase diagram, as presented in Figure 1b. Hypothetically, such a diagram would exist in a solvent where solubilities of caffeine and maleic acid are of the same order of magnitude, and the highest possible in order to promote spontaneous crystallization. The effect the choice of solvent has on the selective growth of a single desired phase of stoichiometric cocrystals was also illustrated by Seaton et al.,[35] studying the benzoic acid/isonicotinamide system in different solvents. They

dx.doi.org/10.1021/cg201581z | Cryst. Growth Des. XXXX, XXX, XXX−XXX

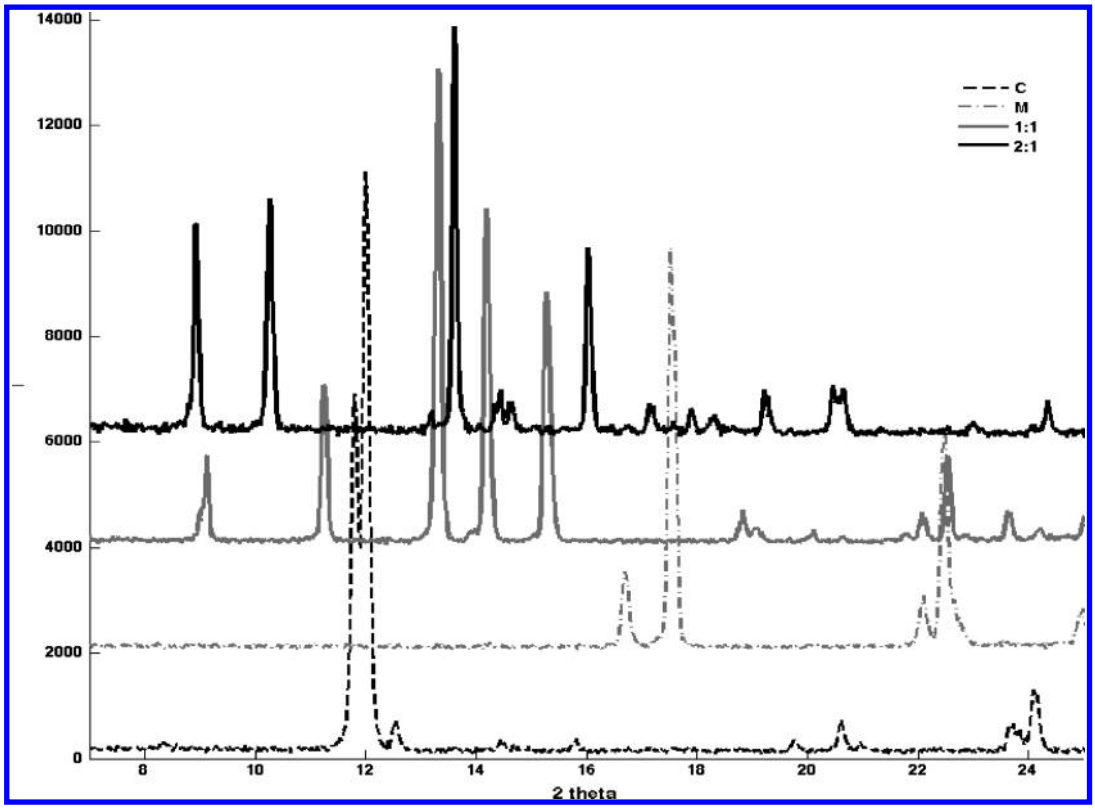

Figure 5. XRPD of caffeine (C), maleic acid (M), 2:1 (samples 2 and 5), and 1:1 (samples 1, 3 and 6) cocrystals.

emphasized the importance of solvent−solute interactions for the preferential formation of one phase over the other, and also suggested the use of a solvent showing comparable solubility toward both components to avoid strongly skewed phase diagrams.

For the purpose of this work, ethyl acetate was selected as a crystallization solvent. Compared to acetone, ethyl acetate shows a higher solubility toward caffeine, and more importantly, the relative solubility of maleic acid vs caffeine is reduced from 40 to an approximate value of 7. (The relative solubility is obtained by comparing the molar solubility of both components in solution. Ideally, one could argue that this value should be even further reduced in favor of caffeine, but for the purpose of this work, reproducible crystallization of the 2:1 phase, it is sufficient for the nucleation of this phase to be kinetically favored.) By using this solvent we hoped to obtain a more symmetric phase diagram and render the 2:1 zone more easily accessible.

Kinetic Screening. As mentioned above, our goal is to obtain a reproducible crystallization of the 2:1 phase in solution with crystals large enough for structural analysis. To identify the zones, for which the 2:1 phase is in equilibrium with a liquid phase, one would ideally define the entire ternary phase diagram or determine the thermodynamic constants mentioned above at a given temperature. This can however be quite time-consuming, and recently alternative phase diagrams have been developed, which allow a rapid identification of the regions in which cocrystal phases are stable. These phase diagrams are constructed based on the principle that if a cocrystal is more stable in solution than its components, its solubility (representing the free energy of formation) will be lower than the combination of its constitutents, provided an appropriate solvent has been selected.[36] Using the relative solubilities of both components as a starting point (point P in Figure 2),[37] diagrams as presented in Figure 2 for a 1:1 and a stoichiometrically diverse cocrystal system can be constructed.[38,39]

As shown in these phase diagrams, a solution saturated in both components is likely to be supersaturated with respect to the cocrystal phase (point P in Figure 2a). Although these diagrams are thermodynamic diagrams, one could nevertheless expect an increased probability toward spontaneous crystallization for compositions similar to that of point P.

We therefore decided to design an experimental screening plan around point P (Figure 2a). (The initial reference point is chosen as the center of an experimental plan, consisting of 10 mol % increase and/or decrease of component concentrations.) This screen is clearly different from classical screening methods, as one no longer focuses on stoichiometric ratios of both components but rather on saturation concentrations of both components. Indeed, a recent contribution showed that solution concentration is of great importance for the outcome of the stoichiometrically diverse caffeine/*p*-hydroxybenzoic acid cocrystal system.[40] As temperature is an important parameter in a phase diagram, the experiment plan was created at two different reference temperatures, 35 and 55 °C. To identify the central point P at both temperatures, solubility curves of caffeine and maleic acid as a function of temperature were determined using the multiwell scanning device. Both curves are shown in Figure 3.

Screening samples (Table 1) were prepared by dissolving compounds at higher temperature and storing the samples at the reference temperature for spontaneous crystallization. However, at this temperature, no spontaneous crystallization was observed after 48 h, most likely due to relatively low supersaturation levels. As we were looking for a fast method for

dx.doi.org/10.1021/cg201581z | *Cryst. Growth Des.* XXXX, XXX, XXX−XXX

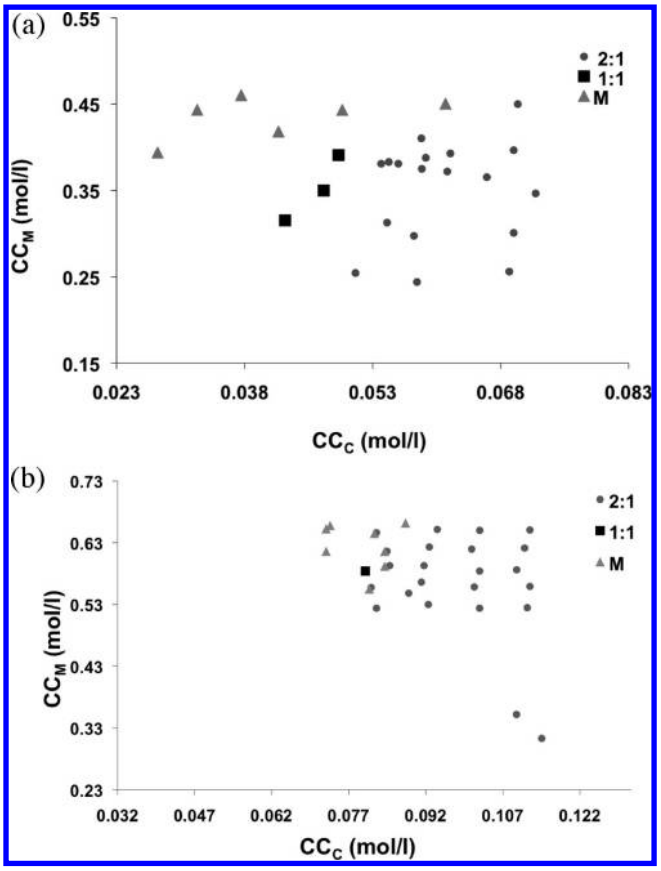

Figure 6. Extended screen for solid phases obtained from spontaneous crystallization (a) at 10 °C (b) at 20 °C. Origin is set at the solubility of caffeine and maleic acid, input concentration of caffeine (cc_C) on the *x*-axis and input concentration of maleic acid (cc_M) on the *y*-axis, (a) at 10 °C (b) at 20 °C.

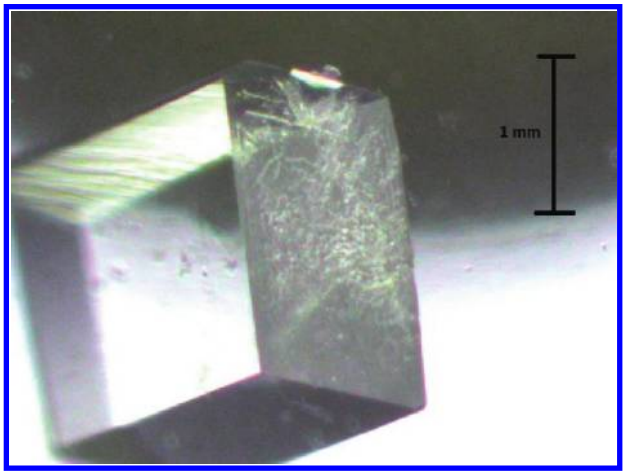

Figure 7. OM image of the 1:1 phase II cocrystal.

spontaneous crystallization of the 2:1 phase in solution, we decided to decrease the induction time by lowering the sample temperature, thus increasing supersaturation. The samples created for a reference temperature of 35 and 55 °C were kept at 10 and 20 °C, respectively. Under the assumption that the solubilities of both cocrystal components decrease symmetrically, we expected the cocrystal stability zones of the phase diagram at lower temperature to be screened. At these temperatures, spontaneous crystallization occurred in most of the vials. (Samples were analyzed from the moment spontaneous crystallization occurred. After 48 h, spontaneous crystallization had occurred in almost all of the vials.)

Optical microscopy (OM), using the inverted microscope scanning device, showed various needle-like crystal habits in solution for the different vials, as shown in Figure 4. Although initial solution concentrations are relatively similar, the thickness of the obtained crystals strongly varies from one sample to another. Differences in crystal habit can be indicative of differences in solid phase, but should not be taken as sole proof, as the final crystal habit depends on nucleation and growth kinetics.

All samples were therefore filtered and analyzed by XRPD using both caffeine and maleic acid, as reference sperctra, as well as the XRPD of 1:1 and 2:1 cocrystals obtained by grinding.[41] As shown in Figure 5, the diffractograms strongly differ for values of 2θ ranging between 5 and 30°, allowing for a straightforward identification of the different solid phases.

XRPD analysis showed three samples to contain maleic acid, three samples to contain the 1:1 cocrystal, and three to contain the 2:1 cocrystal. To our knowledge, it is the first time that spontaneous crystallization of the 2:1 cocrystal phase in solution is reported. As shown in Figure 4, maleic acid and the 1:1 cocrystal show a thick needle-shaped habit, but the 2:1 cocrystal shows a fine needle-shaped habit comparable to that of caffeine.[42]

To confirm our results and show the reproducibility of the crystallization conditions, the initial experimental plan was enlarged to cover an extended zone around the central point. (Samples were prepared in a similar manner to the intital screen. Analysis was performed at latest 24 h after spontaneous crystallization of a sample occurred. The composition of the different samples can be found in the Supporting Information.) Figure 6 shows the results of this screen, taking the solubility of caffeine and maleic acid respectively at 10 and 20 °C as the point of origin for the plots. No spontaneous crystallization was observed after a 1 month isothermal hold at 20 °C, for compositions with $cc_M < 0.53$ and $cc_C < 0.07$ mol/L.

As expected, maleic acid crystallizes spontaneously, when concentrations in maleic acid are relatively high and caffeine concentrations are low. In none of the screening conditions considered, caffeine crystallized out spontaneously. Figure 6 shows the majority of the samples to lead to successful cocrystallization of the 2:1 cocrystal, implying that under the conditions considered here, the hetero-intermolecular interactions (maleic acid/caffeine) are likely to be stronger than the homo-intermolecular interactions (maleic acid/maleic acid and caffeine/caffeine). The strong tendency for spontaneous 2:1 cocrystallization in ethyl acetate confirms our hypothesis that the nature of the solvent is crucial for the crystallization of stoichiometrically diverse cocrystals. Furthermore, the extended screen shows a remarkable reproducibility of the spontaneous crystallization of this phase in solution. Figure 6 is a kinetic diagram showing the zones of spontaneous nucleation for the different phases.

The spontaneous crystallization of the 2:1 cocrystal phase led to crystals suitable for single crystal XRD. We are the first to obtain single crystals suitable for structural analysis and hence to report the structure of the 2:1 cocrystal.

Furthermore, sample 8 of the initial screen led to the spontaneous crystallization of a hithertho unknown polymorph of the 1:1 cocrystal (Figure 7) as determined by single crystal X-ray diffraction (Figure 11) and powder Xray diffraction

dx.doi.org/10.1021/cg201581z | *Cryst. Growth Des.* XXXX, XXX, XXX–XXX

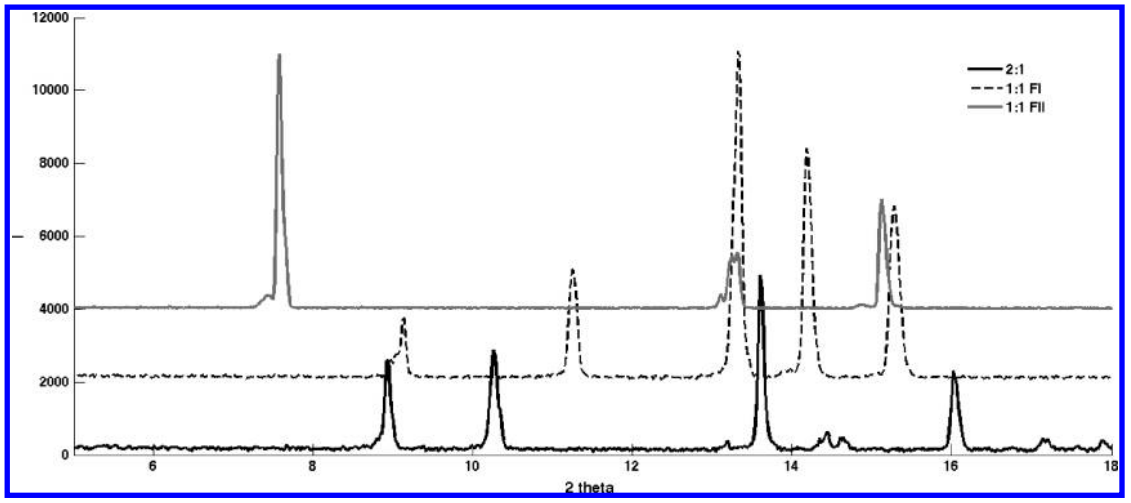

Figure 8. XRPD comparison of 2:1, 1:1 (FI), and 1:1 (FII) cocrystals.

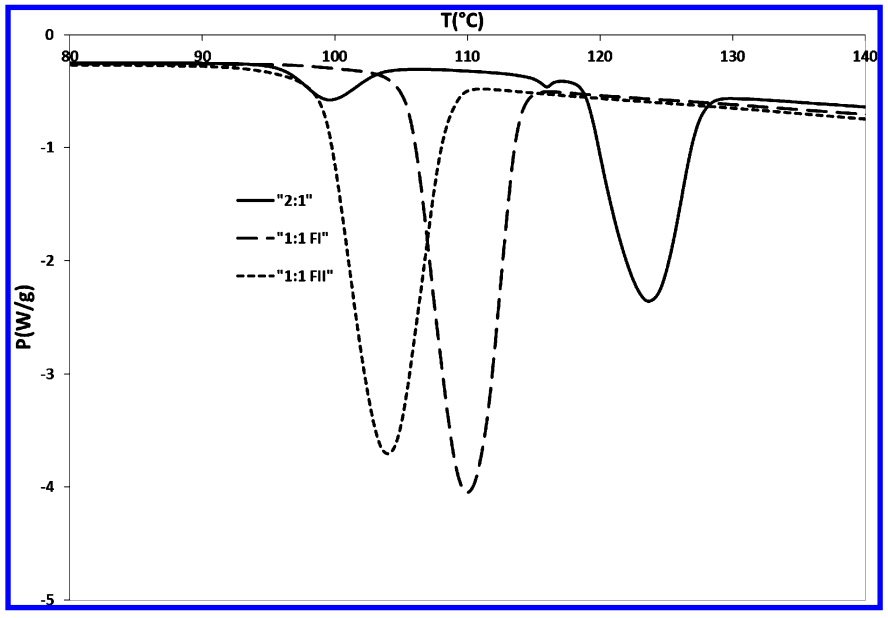

Figure 9. DSC thermogram, presenting the heat flow as a function of the sample temperature.

Table 2. Crystallographic Data for Cocrystals 1:1 (FI), 1:1 (FII), and 2:1

cocrystals	1:1 (FI) (ref 4)	1:1 (FII)	2:1
structural formula	$(C_8H_{10}N_4O_2)(C_4H_4O_4)$	$(C_8H_{10}N_4O_2)(C_4H_4O_4)$	$2*[(C_8H_{10}N_4O_2)_2(C_4H_4O_4)]$
formula weight (g/mol)	310.26	310.26	504.45
crystal system	monoclinic	triclinic	monoclinic
space group	$P2_1/n$	$P\bar{1}$	Pc
a (Å)	6.8565(2)	7.9765(18)	13.1974(3)
b (Å)	12.5051(4)	8.067(3)	6.9662(2)
c (Å)	15.8362(5)	12.162(5)	26.2816(8)
α (°)	90	77.59(3)	90
β (°)	93.6100(10)	77.68(3)	97.847(1)
γ (°)	90	69.92(3)	90
V (Å^3)	1355.12	709.44	2393.59
Z	4	2	2
ρ_{calc} (g/cm^3)	1.521	1.453	1.399
R-factor	N.A.	5.91	9.73

(Figure 8). Although identification and characterization of polymorphism is nowadays fairly common for small organic compounds of pharmaceutical interest, polymorphism of cocrystals remains a less studied topic,[43,44] mainly due to the difficulties encountered when screening for polymorphs of multicomponent crystals.[45] However, the appearance of a

dx.doi.org/10.1021/cg201581z | Cryst. Growth Des. XXXX, XXX, XXX−XXX

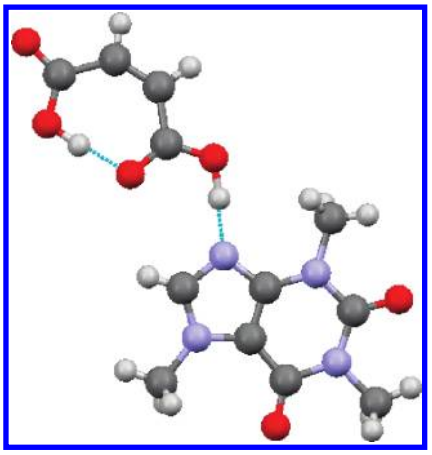

Figure 10. Dimeric caffeine–maleic acid unit, as observed in the 1:1 FI cocrystal (ref 23).

polymorph on later stages of product development could have a substantial impact from a biological as well as legal point of view. The second polymorph of the 1:1 cocrystal, called phase II hereafter, shows a cubic habit (Figure 7). The XRPD pattern (Figure 8) is clearly distinct from the pattern observed for the 1:1 and 2:1 cocrystals.

The new polymorph is stable in solution for over a month and can be regrown from solution upon seeding with tiny amounts of the initial crystal. However, this polymorph was not found to crystallize spontaneously in any of the other instances, once more highlighting the difficulties when screening for polymorphic phases of cocrystals.

Thermal Analysis. DSC analyses were performed on the cocrystal substances, as well as the single component starting materials. As shown in Figure 9, all of the cocrystal compounds show a clear single melting peak. Maleic acid and caffeine show melting onsets at respectively 139 and 236 °C (see Supporting Information Figure S.1). The maleic acid thermogram shows a degradation endotherm following the melting endotherm.

All of the cocrystals show lower melting temperatures, with the 2:1 compound showing an onset at 119 °C and the 1:1 cocrystal showing an onset at 99 and 105 °C for FII and FI respectively. (The small endothermic signal at 100 °C for the 2:1 cocrystal could be due to a small contamination with the 1:1 cocrystal phase during the isolation of the 2:1 phase from solution.) As for maleic acid, the melting endotherm is followed by a degradation endotherm for all compounds.

The relative stability of the two polymorphs of the 1:1 cocrystal was studied placing single crystals of FI and FII in a ethyl acetate solution at 18 °C. [The solution was created to ensure the 1:1 phase is stable in solution (caffeine = 0.060 $mol{\cdot}L^{-1}$; maleic acid = 0.215 $mol{\cdot}L^{-1}$).] The FII crystal dissolved slowly over a one week time period, in favor of the FI crystal. As FII also shows a lower melting temperature, the two polymorphs are monotropically related between 18 and 98 °C, with FI being the most stable phase.

Structural Analysis. The crystallographic parameters for the 1:1 (FI and FII) and 2:1 cocrystals are shown in Table 2.

The crystallographic parameters for each cocrystal that were identified are displayed in Table 2. FI shows the highest density, as can be expected, for the most stable polymorph. The 2:1 cocrystal shows the lowest density.

Caffeine–Maleic Acid (1:1) (FI) (Figure 10). The main structural characteristics of the 1:1 FI cocrystal are given here. A more detailed description is given in ref 23 (CSD Refcode GANYEA).

The cis-orientation of both carboylic groups of maleic acid predisposes this compound to form an intramolecular $[S^1_1(7)]$ hydrogen bond as observed in the 1:1 cocrystal.[46,47] This intramolecular hydrogen bond is conserved in the cocrystal. Dimeric caffeine–maleic acid units are formed by the expected intermolecular $[R^2_2(7)]$ heterosynthon. Translation and 2_1-

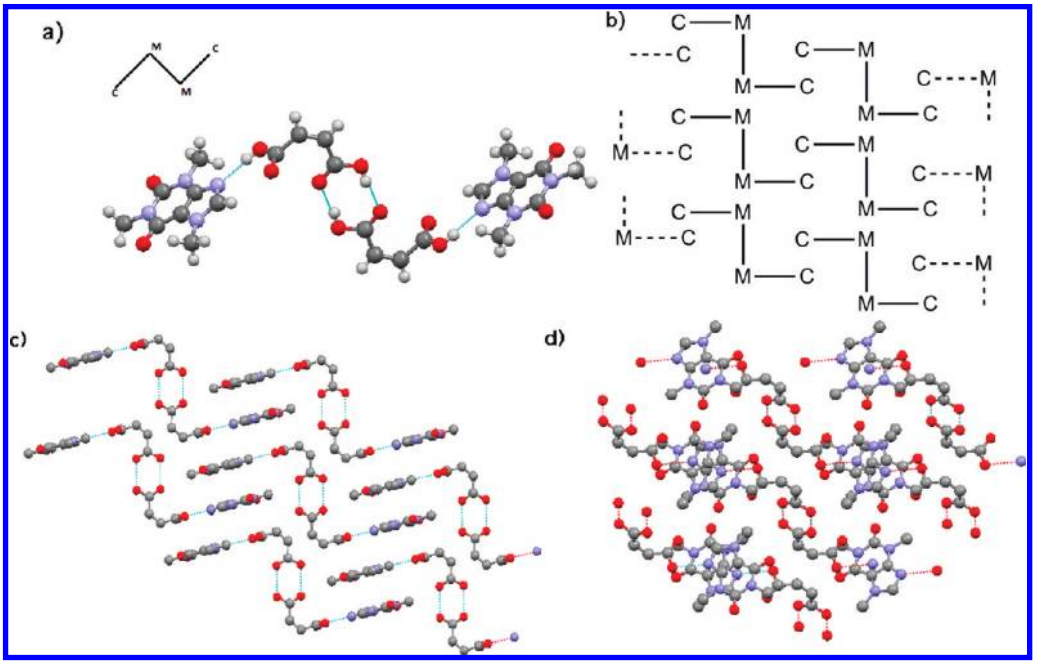

Figure 11. (a) Four components strand showing the caffeine/maleic acid heterosynthon, and the maleic acid/maleic acid homosynthon. (b) Schematic drawing of the strands packing together in a planar structure. (c) Planar structure, $(10\bar{1})$ plane (hydrogens omitted for clarity). (d) Planes are repeated through translation in the direction of the diagonal of the *ac* plane (hydrogens are omitted for clarity).

dx.doi.org/10.1021/cg201581z | *Cryst. Growth Des.* XXXX, XXX, XXX–XXX

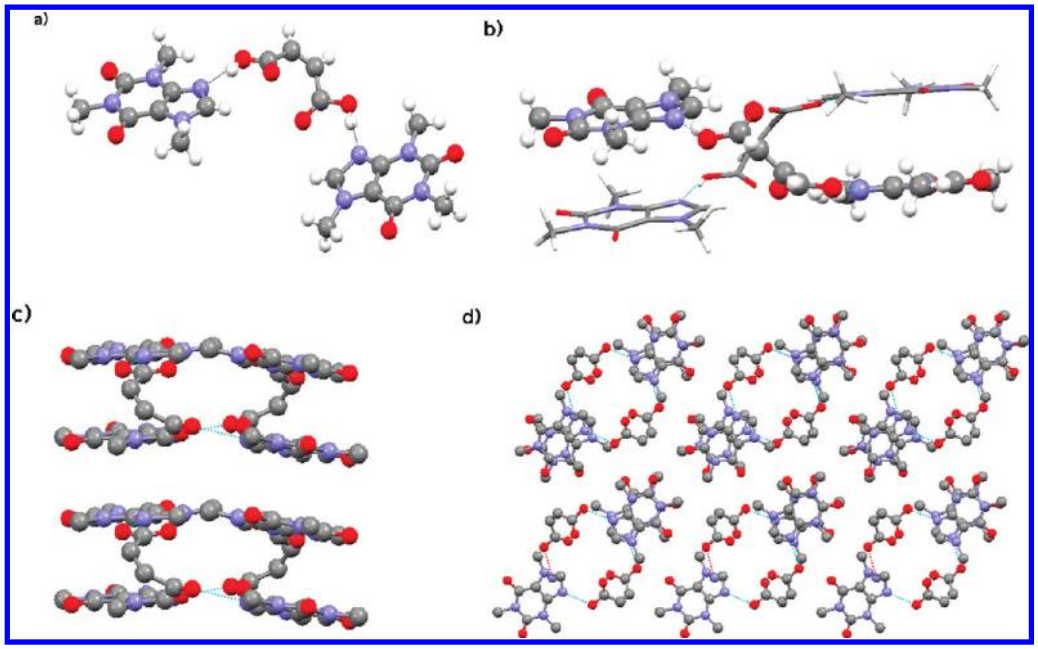

Figure 12. (a) Three components strand showing a maleic acid molecule linking with two caffeine molecules. (b) Crab-claw like pinching of two such strands, leading to a repeating unit; (c) Column along the *b* axis, by stacking the repeated unit of panel c. (d) Columns stacked along each other.

screw axis symmetry leads to the formation of two-dimensional *bc* plane sheets, propagated in the *a* axis direction via the n glide plane.

No other hydrogen bonding is observed in the crystal packing.

Caffeine–Maleic Acid (1:1) (FII) (Figure 11). The caffeine–maleic acid 1:1 (FII) cocrystal crystallizes in a triclinic system with space group $P\bar{1}$ and with cell parameters a = 7.9765(18) Å, b = 8.067(3) Å, c = 12.162(5) Å, α = 77.6°, β = 77.7°, and γ = 69.9°. The unit cell contains two caffeine and two maleic acid molecules.

This polymorph no longer shows an intramolecular hydrogen-bonding motif for maleic acid. The motif is broken by the O–C–C–C torsion of about 80°. This carboxylic acid group forms the expected intermolecular $[R^2_2(7)]$ heterosynthon with caffeine, leading to a dimeric maleic acid–caffeine unit. Two such dimeric units are connected through a $[R^2_2(8)]$ homosynthon between two carboxylic acid groups of adjacent units, leading to a final four components strand as shown in Figure 11a.

On the whole, these strains stack one onto another in the direction of the *b* axis. Two parallel strands overlap (Figure 11b), to form a planar structure. These two-dimensional planes are repeated by a translation in the $[10\bar{1}]$ direction (Figure 11d).

Although a strong COOH $[R^2_2(8)]$ homosynthon is formed, the breaking of the planar structure of maleic acid to predispose this molecule for two intramolecular bonds could in part explain the reduced stability of this polymorphic phase. Furthermore, the latter phase only shows three hydrogen bonding synthons for a 2*(maleic acid/caffeine) motif, where four synthons (2*2) are observed for polymorph I. The deformation of the maleic acid component could also explain the lower density. The N---(H)O distance is furthermore increased from 2.51 Å in phase I to 2.73 Å in phase II, possibly indicating a less strongly bonded $[R^2_2(7)]$ heterosynthon for the latter.

The experimental XRPD diffractogram obtained after grinding matches the simulated diffractogram derived from the single crystal structure.

Caffeine–Maleic Acid (2:1). The caffeine–maleic acid 2:1 (Figure 12) cocrystal crystallizes in a monoclinic system with space group *Pc* and with cell parameters a = 13.1974(3) Å, b = 6.9662(2) Å, c = 26.2816(8) Å, $\alpha = \gamma$ = 90.0°, and β = 97.8°. The unit cell contains two units of a dimeric 2:1 caffeine–maleic acid strand, leading to a total of eight caffeine molecules per unit cell.

As for the 1:1 (FII) polymorph intramolecular hydrogen bonding is not observed for maleic acid. Contrary to this phase, not one but both of the carboxylic acid groups are twisted out of the molecular plane, leading to an unstable arrangement for maleic acid. However, this particular arrangement allows for the formation of two intermolecular $[R^2_2(7)]$ heterosynthons (Figure 12a), as expected in the earlier work of Trask et al. (Scheme 2).[22] Two such strands come together like the claws of a crab clicking one into the other (Figure 12b). The final unit cell contains another of these motifs, which is the mirror image of the first motif.

Repeated stacking of similar units leads to a final columnar structure along the *b* axis (Figure 12c). Stacking of the mirror image motifs leads to a helical column structure with opposite screw sense. The maleic acid molecule in the 2:1 cocrystals strongly deforms to accommodate the possibility to link two caffeine molecules. This possibility explains the lower density of this compound. Furthemore, this deformation would account for a less strongly bonded $[R^2_2(7)]$ heterosynthon as indicated by the N---(H)O distance of 2.98 Å.

The experimental XRPD diffractogram obtained after grinding matches the simulated diffractogram derived from the single crystal structure.

The crystal structure of the 2:1 cocrystal shows the importance of the $[R^2_2(7)]$ heterosynthons as it is the only hydrogen bonding motif to be present for this structure.

dx.doi.org/10.1021/cg201581z | *Cryst. Growth Des.* XXXX, XXX, XXX–XXX

CONCLUSION

In this contribution we showed the importance of the solvent selection and its effect on the synthesis of stoichiometrically diverse cocrystals, using kinetic screening methods based on the relative solubilities (in the selected solvent) of both components of cocrystal as a starting point. Focusing on the caffeine/maleic acid system, we showed the 2:1 cocrystal zone to become accessible in an ethyl acetate solution, hereby being the first to report a reproducible spontaneous crystallization of the 2:1 phase in solution. Compared to acetone, the relative maleic acid/caffeine solubility is reduced from 40 to 7, thereby promoting the nucleation of the 2:1 phase. Furthermore, during the application of screening conditions a polymorph of the 1:1 cocrystal was identified. Structures of both compounds were resolved by XRD analysis and show breaking of the intramolecular hydrogen bond of maleic acid, in favor of the formation of intermolecular heterosynthons.

The choice of solvent is therefore of great importance for cocrystal identification in solution, with an increased possibility of observing different stoichiometric phases for solvents showing comparable solubility toward both cocrystal components.

ASSOCIATED CONTENT

Supporting Information

CIF files for the 2:1 cocrystal (CCDC No. 844797) and the 1:1 (FII) cocrystal (CCDC No. 844798). Supplementary DSC analysis of maleic acid and caffeine (Figure S.1). The different compositions of the extended screen (Table S.1). This material is available free of charge via the Internet at http://pubs.acs.org.

AUTHOR INFORMATION

Corresponding Author

*Tel: +32 10 47 2811. Fax: +32 10 47 27 07. E-mail: Tom.leyssens@uclouvain.be. Web: http://www.uclouvain.be/leyssens-group.

ACKNOWLEDGMENTS

We would like to thank Dr. V. Heresanu for his help with the XRPD analyses, and Dr. M. Giorgi and Dr. K. Robeyns for the single crystal analysis of respectively the 2:1 and 1:1 (FII) cocrystals. T.L. is also grateful for the financial support of the F.N.R.S.

REFERENCES

(1) Cheney, M. L.; Weyna, D. R.; Shan, N.; Hanna, M.; Wojtas, L; Zaworotko, M. J. *J. Pharm. Sci.* **2011**, *100*, 2172−2181.
(2) Schultheiss, N.; Newmann, A. *Cryst. Growth Des.* **2009**, *9*, 2950−2967.
(3) Shan, N.; Zaworotko, M. J. *Drug Discovery Today* **2008**, *13*, 440−446.
(4) Trask, A. V.; Jones, W. *Top. Curr. Chem.* **2005**, *254*, 41−70.
(5) Springuel, G.; Norberg, B.; Robeyns, K.; Wouters, J.; Leyssens, T. *Cryst. Growth Des.* **2011**, in press.
(6) Almarsson, Ö.; Zaworotko, M. J. *J. Chem. Commun.* **2004**, *188*, 9−1896.
(7) Gagnière, E.; Mangin, D.; Puel, F.; Valour, J.-P.; Klein, J.-P.; Monnier, O. *J. Cryst. Growth* **2011**, *316*, 118−125.
(8) Gagnière, E.; Mangin, D.; Puel, F.; Bebon, C.; Klein, J.-P.; Monnier, O.; Garcia, E. *Cryst. Growth Des.* **2009**, *9*, 3376−3383.
(9) Griesser, U. J.; Burger, A. *Int. J. Pharm.* **1995**, *120*, 83−93.
(10) Edwards, H. G. M.; Lawson, E.; De Matas, M.; Shields, L.; York, P. J. *Chem. Soc., Perkin Trans. 2* **1997**, 1985−1990.
(11) Mercer, A.; Trotter, J. *Acta Crystallogr.* **1978**, *B34*, 450−453.
(12) Leger, J. M.; Alberola, S.; Carpy, A. *Acta Crystallogr.* **1977**, *B33*, 1455−1459.
(13) Ghosh, M.; Basak, A. K.; Mazumdar, S. K.; Sheldrick, B. *Acta Crystallogr.* **1991**, *C47*, 577−58.
(14) Craven, B. M.; Gartland, G. L. *Acta Crystallogr.* **1974**, *B30*, 1191−1195.
(15) Das, B.; Baruah, J. B. *Cryst. Growth Des.* **2011**, *11*, 278−286.
(16) Habgood, M.; Price, S. L. *Cryst. Growth Des.* **2010**, *10*, 3263−3272.
(17) Friscic, T.; Trask, A. V.; Jones, W.; Motherwell, W. D. S. *Angew. Chem., Int. Ed.* **2006**, *45*, 7546−7550.
(18) Karki, S.; Fricic, T.; Jones, W.; Motherwell, W. D. S. *Mol. Pharmaceutics* **2007**, *4*, 347−354.
(19) Friscic, T.; Trask, A. V.; Motherwell, W. D. S.; Jones, W. *Cryst. Growth Des.* **2008**, *8*, 1605−1609.
(20) Martin, R.; Lilley, T. H.; Bailey, N. A.; Flashaw, C. P.; Haslam, E.; Magnolato, D.; Begley, M. J. *Chem. Commun.* **1986**, 105.
(21) Bucar, D. K.; Henry, R. F.; Lou, X.; Duerst, R. W.; Borchardt, T. B.; MacGillivray, L. R.; Zhang, G. G. Z. *Mol. Pharmaceutics* **2007**, *4*, 339−346.
(22) Trask, A. V.; Motherwell, W. D.; Jones, W. *Cryst. Growth Des.* **2005**, *5*, 1013−1021.
(23) Guo, K.; Sadiq, G.; Seaton, C.; Davey, R.; Yin, Q. *Cryst. Growth Des.* **2010**, *10*, 268−273.
(24) Bothe, H.; Cammenga, H. K. *Thermochim. Acta* **1980**, *40*, 29−39.
(25) Lehto, V.-P.; Lain, E. *Thermochim. Acta* **1998**, *317*, 47−58.
(26) *Nonius (2001). COLLECT*; Nonius BV: Delft, The Netherlands, 2001.
(27) Otwinowski, Z.; Minor, W. Macromolecular Crystallography, Part A. *Methods in Enzymology*; Carter, C. W., Jr., Sweet, R. M., Eds.; Academic Press: New York, 1997; Vol. *276*, pp 307−326
(28) Sheldrick, G. M. *Acta Crystallogr.* **2008**, *A64*, 112−122.
(29) Detoisien, T.; Forite, M.; Taulelle, P.; Teston, J.; Colson, D.; Klein, J. P.; Veesler, S. *Org. Process Res. Dev.* **2009**, *13*, 1338−1342.
(30) Aher, S.; Dhumal, R.; Mahadik, K.; Paradkar, A.; York, P. *Eur. J. Pharm. Sc.* **2010**, *41*, 597−602.
(31) Alhalaweh, A.; George, S.; Boström, D.; Velaga, S. P. *Cryst. Growth Des.* **2010**, *10*, 4847−4855.
(32) Qun, Y.; Chow, P. S.; Tan, R. B. H. *Cryst. Growth Des.* **2010**, *10*, 2383−2387.
(33) Jayasankar, A.; Sreenivas Reddy, L.; Bethune, S. J.; Rodriguez-Hornedo, N. *Cryst. Growth Des.* **2009**, *9*, 889−897.
(34) Ainouz, A.; Authelin, J.-R.; Billot, P.; Lieberman, H. *Int. J. Pharm.* **2009**, *374*, 82−89.
(35) Seaton, C. C.; Parkin, A.; Wilson, C. C.; Blagden, N. *Cryst. Growth Des.* **2009**, *9*, 47−56.
(36) Nehm, S. J.; Rodriguez-Spong, B.; Rodriguez-Hornedo, N. *Cryst. Growth Des.* **2006**, *6*, 592−600.
(37) Chiarella, R. A.; Davey, R. J.; Peterson, M. L. *Cryst. Growth Des.* **2007**, *7*, 1223−1226.
(38) Ter Horst, J. H.; Deij, M. A.; Cains, P. W. *Cryst. Growth Des.* **2009**, *9*, 1531−1537.
(39) Gagnière, E.; Mangin, D.; Puel, F.; Rivoire, A.; Monnier, O.; Garcia, E.; Klein, J. P. *J. Cryst. Growth* **2009**, *311*, 2689−2695.
(40) He, G.; Chow, P. S.; Tan, R. B. H. *Cryst. Growth Des.* **2010**, *10*, 3763−3769.
(41) Friscic, T.; Jones, W. *Cryst. Growth Des.* **2009**, *9*, 1621−1637.
(42) Sarfraz, A.; Simo, A.; Fenger, R.; Christen, W.; Rademann, K.; Panne, U.; Emmerling, F. *Cryst. Growth Des.* **2011**, DOI: 10.1021/cg101358q.
(43) Aitipamula, S.; Shan Chow, P.; Tan, R. B. H. *Cryst. Growth Des.* **2010**, *10*, 2229−2238.
(44) ter Horst, J. H.; Cains, P. W. *Cryst. Growth Des.* **2008**, *8*, 2537−2542.
(45) Rager, T.; Hilfiker, R. *Cryst. Growth Des.* **2010**, *10*, 3237−3241.
(46) James, M. N. G.; Williams, G. J. B. *Acta Crystallogr.* **1974**, *B30*, 1249−1257.

(47) Day, G. M.; Trask, A. V.; Motherwe ll, W. D. S.; Jones, W. *Chem. Commun.* **2006**, 54−56.